SAND--89-1607C

DE90 000789

NEW DEVICES USING FERROELECTRIC THIN FILMS

C. E. Land, M. A. Butler and S. J. Martin

Sandia National Laboratories
Albuquerque, New Mexico 87185

ABSTRACT

Recent developments in the fabrication technologies of ferroelectric thin films in general and of PZT (lead zirconate titanate) and PLZT (lead lanthanum zirconate titanate) thin films in particular have suggested the feasibility of several new devices. Integrated optical devices for information processing and high-speed switching, high-density optical information processing and storage devices and spatial light modulators are some of the applications currently being investigated for these films. Ongoing studies of the longitudinal electrooptic effects and the photosensitivities of PZT and PLZT thin films have established the feasibility of erasable/rewritable optical memories with fast switching and potentially long lifetimes compared to current magneto-optic thin film devices. Some properties of PZT thin films and of new devices based on those properties are described in this paper.

INTRODUCTION

Since 1983 researchers have been fabricating transparent PZT and PLZT ferroelectric thin films on a variety of substrates (1-5). These films have excellent ferroelectric, electrooptic and piezoelectric properties. Several novel optical devices based on light propagation in the plane of the films (i.e., in channeled waveguide structures) have been demonstrated (6-9). Radiation-hard, ferroelectric, nonvolatile memory devices have also been demonstrated. More recently, we have demonstrated the feasibility of PZT or PLZT high-density optical information storage and processing devices based on the longitudinal electrooptic properties of these materials (10-12). The application of ferroelectric thin films to optical information storage and processing devices depends first on their capability to store optical information, i.e., their intrinsic and/or extrinsic photosensitivities, and then upon the capability of reading the stored information with a reasonable signal-to-noise ratio. The latter capability depends essentially upon the magnitude of the longitudinal electrooptic coefficients of the films. We have developed techniques for measuring the longitudinal electrooptic coefficients (10), and the results of some of the preliminary measurements are included in this paper. Techniques for evaluating photosensitivities of thin films are based on measuring the photocurrent generated rather than the reduction in coercive voltage (used previously for bulk ceramics) when the film is exposed to light (10,11).

This paper briefly discusses PZT and PLZT longitudinal electrooptic effects, photosensitivities, photocurrent generation characteristics and some proposed devices which will use these properties. The compatibility of ferroelectric film fabrication techniques with current semiconductor processing technology should permit rapid development of these new devices.

LONGITUDINAL ELECTROOPTIC EFFECTS

The longitudinal electrooptic coefficients are a measure of the change in birefringence as a function of applied electric field with the field applied normal to the surface of the film. The change in birefringence was measured as the polarization of the film was switched through the P vs. V hysteresis loop. Since the optic axis of a polycrystalline ferroelectric film, like the related bulk ceramic material, aligns in a direction approximately coincident with the applied electric field, and the film has infinite rotational symmetry in the plane normal to the optic axis, measurement of birefringence with a longitudinal field can be achieved only if the film is rotated by some finite angle with respect to the measuring light beam. For the results reported in this paper, the configuration of the experimental sample is similar to that shown in Fig. 1. The film substrate consists of a silicon wafer with a platinum-film base electrode deposited on the top surface. A PZT 50/50 (50 mole percent $PbZrO_3$ and 50 mole percent $PbTiO_3$) film is deposited, using a sol-gel technique (5) on the platinum base electrode, and a thin gold electrode (~200 Angstroms thick) is deposited over the PZT. Two PZT 50/50 films, one 0.5 μm thick and the other 1 μm thick, were used for the measurements reported below. The sample was rotated as follows: starting with the surface normal aligned with the light beam, the sample was rotated by 45° about the vertical axis to achieve a 45° angle between the light beam and the surface normal in the horizontal plane. A schematic of the experimental configuration for the electrooptic measurements is shown in Fig. 2.

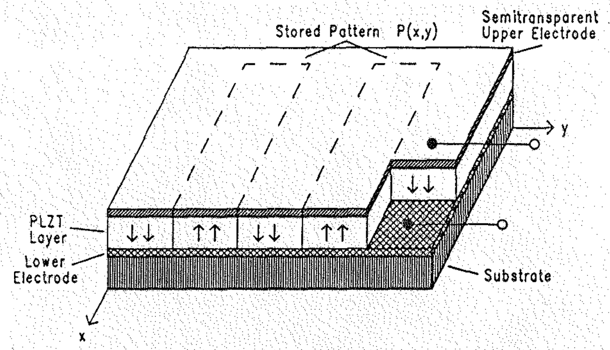

Fig.1. Configuration of ferroelectric thin-film storage and processing devices. The ferroelectric optical image comparator (FOIC) (12) is used for analogue generation of the dot product between a stored image and one projected onto its surface. Arrows indicate orientation of the ferroelectric polarization for a stored bar pattern.

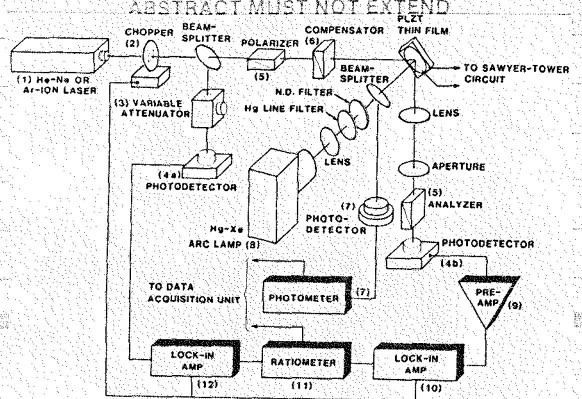

Fig. 2. Schematic of the instrumentation for measuring phase retardation and photosensitivity.

While the film was switched through the P vs. V hysteresis loop (run at 25 mHz or 40 seconds per loop), beginning at $P=-P_R$ (negative saturation remanence) and V=0, the intensity of the laser light reaching photodetector 4b of Fig. 2 through the crossed polarizer-analyzer configuration was governed by the change in birefringence of the PZT film. The relationship between transmittance and retardation is given by

$$T = \sin^2 [\Gamma(0) + \Gamma(V)]/2 \qquad (1)$$

In Eq. (1) above, T is the transmittance I/I_{max}, $\Gamma(0)$ is the pedestal phase retardation at V=0 and $\Gamma(V)$ is the change in phase retardation as the polarization P is switched through the hysteresis loop. Given that the phase retardation expressed in radians is $\Gamma=2\pi L\Delta n$, where L is the light path length in the film, we can calculate Δn using Eq. (1) as follows

$$\Delta n = (\lambda/\pi L) \sin^{-1} [T(0)+T(V)]^{1/2} \quad . \qquad (2)$$

In Eq. (2), T(V) is the change in transmittance with applied voltage and T(0) is the transmittance at $P=-P_R$.

Equation (2) was used to calculate birefringence as a function of applied voltage, and the results for the 0.5 μm thick film are plotted in Fig. 3. The large pedestal birefringences at $P=\pm P_R$ (V=0) are attributed to preferred orientation of the film with the optic axis aligned predominantly normal to the film surface.

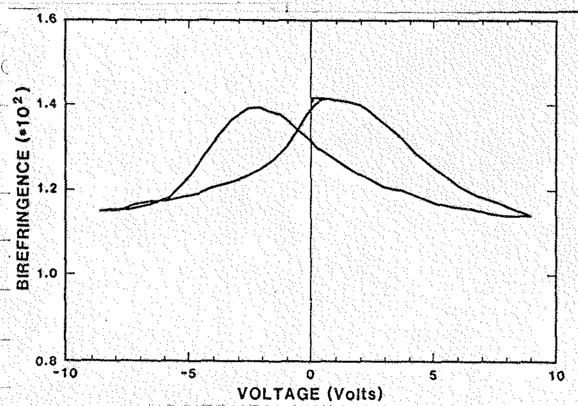

Fig. 3. Birefringence Δn versus V for the 0.5 μm thick PZT 50/50 film.

The data of Fig. 3 can be used to calculate effective quadratic and linear longitudinal electrooptic coefficients for the PZT film. For those segments of the Δn versus V curves where Δn is proportional to E^2, the quadratic electrooptic coefficient R applies, and it is given by

$$R = - 2\, \delta\Delta n/n^3E^2 \quad . \qquad (3)$$

In Eq. 3, $\delta\Delta n$ is the change in birefringence, n is the refractive index of the PZT, E is the electric field V/t and t is the film thickness. In those regions where the Δn versus V curves are approximately linear, the linear longitudinal electrooptic coefficient is given by

$$r_c = - 2\, \delta\Delta n/n^3E \qquad (4)$$

Using Eqs. (3) and (4), we calculated the approximate values of the longitudinal quadratic and linear electrooptic coefficients for both the 0.5 μm and the 1 μm thick films. These values are listed in Table 1.

Table 1. Ferroelectric and Electrooptic Properties of PZT 50/50 Thin Films

	1.0 μm	0.5 μm
P_s ($\mu C/cm^2$)	33.7	14.1
P_r ($\mu C/cm^2$)	8.0	6.1
V_c (volts)	~2.5	~1.5
$\Delta n(0)$ (× 10^2 @514nm)	1.16	1.42
$\Delta n(P_s)$ (× 10^2 @514nm)	0.85	1.14
R (× 10^{17} m^2/V^2)	~1.0	~1.0
r_c (× 10^{11} m/V)	~4.0	~4.0

The results indicate that, although the longitudinal electrooptic coefficients appear to be about a factor of ten smaller than the transverse electrooptic coefficients of bulk ceramics of similar compositions, they are sufficiently high to establish the feasibility of reading stored information by optical techniques.

PHOTOSENSITIVITY

In an effort to evaluate the photosensitivities of PZT thin films, we attempted to use the techniques which we had developed for PLZT ceramics (13). We used the Hg-Xe arc lamp and associated optics shown in Fig. 2 to illuminate the surface of the PZT thin film while we measured the P versus V hysteresis characteristics. We used Hg line filters to achieve approximately monochromatic light, and starting with zero light intensity, we increased the intensity for successive hysteresis curves. As the light intensity increased, the increasing photocurrent effectively masked the reduction in coercive voltage, thus preventing the use of this variable to calculate photosensitivity. Relatively fewer of the photocarriers generated by the illuminating light are trapped in the PZT thin film than in PLZT ceramic wafers. This accounts for the fact that the films are much more efficient photocurrent generators than ceramic wafers of similar compositions, and as a result, we could not evaluate film photosensitivity based on reduction in coercive voltage with increasing illumination.

The photocurrent generated as a function of the illuminating light intensity is related to and can be used to evaluate the photosensitivity of the films. We replaced the integrating capacitor of the Sawyer-Tower circuit with the low-impedance input of a microammeter, and with this circuit we first measured the total current density J_t as the film was switched through a series of hysteresis loops with increasing illumination intensity for each successive loop. We then subtracted the current density for zero illumination from the subsequent data, and the result was approximately the photocurrent density J_{ph}.

Given a fixed exposure time, e.g. one second, we can determine experimentally the photocurrent density J_{ph} threshold for optical information storage in the PZT thin film. When a J_{ph} threshold is measured for one wavelength, we may assume that the same J_{ph} threshold applies for other wavelengths in the near-UV and the visible spectrum. Using the experimentally determined J_{ph} threshold for information storage at 365, 404, 436 and 546 nm wavelengths, we can extract from the J_{ph} vs intensity I data at each of the wavelengths the threshold light intensity I_{th} required for optical information storage (10,11). By multiplying I_{th} by the exposure time, we obtain the threshold exposure energy for information storage at each of the wavelengths. Because the switching speeds of the thin films are very high, we assume reciprocity between exposure time and light intensity applies over some broad range of exposure energies. The reciprocal of the threshold exposure energy expressed in cm^2/erg is equivalent to the ISO standard photosensitivity. In Fig. 4 we have plotted $\log_{10}$ photosensitivity S vs wavelength λ for a 1 second exposure and photocurrent densities J_{ph} of 0.32 $\mu A/cm^2$ and 1.0 $\mu A/cm^2$. The approximate threshold sensitivity is represented by the J_{ph}=0.32 $\mu A/cm^2$ curve.

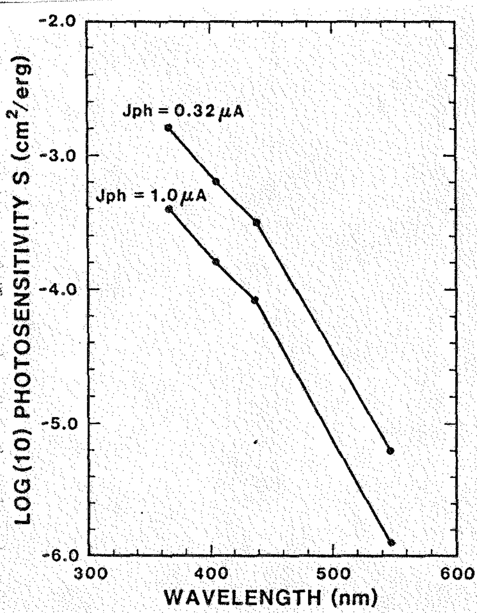

Fig. 4. $\log_{10}$ S (photosensitivity) versus λ (wavelength) for 365, 404, 436 and 546 nm wavelengths.

The photosensitivity of the PZT film is probably at least 10^{-3} cm^2/erg in the near-UV and blue end of the visible, and this is at least a factor of 10^3 higher than for bulk ceramics of similar compositions. The small grain sizes of the films suggest that storage bit sizes of the order of one μm may be feasible.

OPTICAL STORAGE AND PROCESSING DEVICES

Erasable Optical Disk

The results discussed above suggest that the PLZT thin films may be used as the optical information storage media in erasable/rewritable optical disks (14). The recent discovery of a bistable optical storage capability in antiferroelectric (AFE)-phase PLZT ceramics (15) further suggests that a thin film of this material may be particularly useful as the storage medium in erasable/rewritable optical disks. A possible configuration of a PLZT optical disk write/read system is shown in Fig. 5. For AFE compositions which exhibit a field-induced metastable ferroelectric (FE) phase, optical information storage is achieved by first field-inducing the FE phase, applying a biasing field E_B near the knee of the FE-AFE transition threshold, and then exposing the film to the write beam to store digital 1's in the desired bit areas. The FE-AFE transition threshold shifts to a value less than E_B in areas illuminated above the exposure energy threshold. The illuminated areas undergo a transition from the FE to the AFE phase, while the dark areas remain in the FE phase even after removal of the biasing field E_B. Binary information is therefore stored between the metastable FE and the stable AFE phases, and this stored information is nonvolatile. Optical information is stored as a sequence of bits, whose phase is either AFE (a digital 1) or FE (a digital 0).

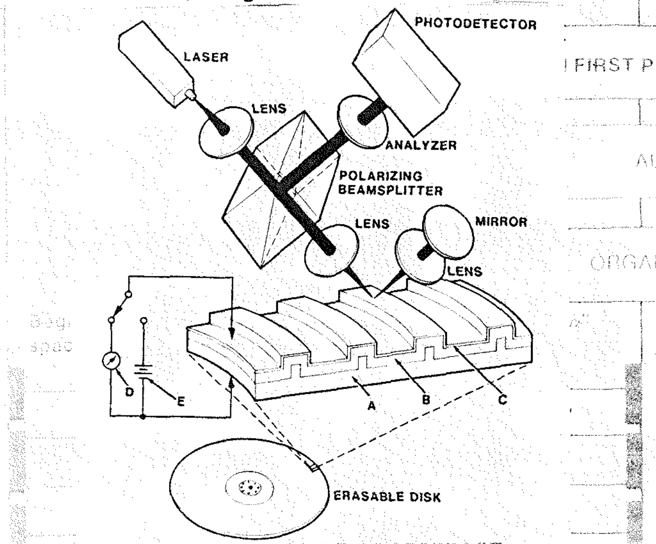

Fig. 5. Erasable optical disk write/read scheme for four light passes through the PLZT thin film. The optical disk consists of: (A) a conductive and reflective substrate or a conductive and reflective film on a rigid substrate; (B) the PLZT thin film and (C) a transparent film top electrode, e.g., indium-tin oxide (ITO). Also shown is: (D) a micro-ammeter for monitoring read photocurrent and (E) a reversible bias voltage supply for switching.

To selectively erase optical information, the polarity of the dc bias voltage is reversed, and the AFE bits to be erased are exposed to the write laser light. New data can then be recorded in the same areas.

In the FE phase the PLZT grains are birefringent, and the optic axes of the domains are preferentially oriented normal to the film surface. In the AFE phase the PLZT is optically isotropic on a macroscopic scale, and there is no FE domain structure. When the read beam encounters a digital 0 (FE phase), its polarization is converted to elliptical and rotated by some angle depending on the birefringence and the film thickness. For a digital 1 (AFE phase), the polarization remains planar and the polarization axis is not rotated. The two phases are easily detected and interpreted as digital 1's or 0's.

Optical Image Comparator

An alternative method of reading stored information has emerged from the photosensitivity measurements and the subsequent photocurrent measurements performed on the PZT films (11). The effective quantum efficiency for generating photocurrents is much higher for the films than for the ceramics, and this introduces the possibility of reading stored information by optical scanning in a manner analogous to electron beam scanning of a vidicon imaging device. The photocurrent generated at the device electrodes provides an accurate electrical readout of the stored optical information. We have used the photocurrent generation capabilities of the thin films to design a ferroelectric optical image comparator (FOIC) (12). When a high resolution image is stored in the thin film of this device, the photocurrent generated by the device represents the dot product of the stored image and a second image projected onto its surface. A schematic diagram of the FOIC is shown in Fig. 1.

REFERENCES

1. H. Adachi, T. Kawaguchi, K. Setsune, K. Ohji and K. Wasa, Electrooptic effects of $(Pb,La)(Zr,Ti)O_3$ thin films prepared by rf planar magnetron sputtering, Appl. Phys. Lett. 42, pp. 867-868, 15 May 1983.
2. S. B. Krupanidhi, N. Maffei, M. Sayer and K. El-Assal, RF planar magnetron sputtering and characterization of ferroelectric $Pb(Zr,Ti)O_3$ films, J. Appl. Phys. 54, pp. 6601-6609, 1983.
3. H. Adachi, T. Mitsuyu, O. Yamazaki and K. Wasa, Ferroelectric $(Pb,La)(Zr,Ti)O_3$ epitaxial thin films on sapphire grown by rf-planar magnetron sputtering, J. Appl. Phys. 60, pp. 736-741, 15 July 1986.
4. H. Adachi, T. Mitsuyu, O. Yamazaki and K. Wasa, Preparation and properties of $(Pb,La)(Zr,Ti)O_3$ epitaxial thin films by multi-target sputtering, Jap. J. Appl. Phys. 24, Supplement 24-3, 1985.
5. K. D. Budd, S. K. Dey and D. A. Payne, Sol-gel processing of $PbTiO_3$, $PbZrO_3$, PZT and PLZT thin films, Brit. Cer. Soc. Proc. 36, pp. 107-121, 1985.
6. K. Wasa, O. Yamazaki, H. Adachi, T. Kawaguchi and K. Setsune, Optical TIR switches using PLZT thin-film waveguides on sapphire, J. Lightwave Tech. LT-2, pp.710,714, 1984.
7. H. Higashino, T. Kawaguchi, H. Adachi, T. Makino and O. Yamazaki, High-speed optical TIR switches using PLZT thin-film waveguides on sapphire, Jap. J. Appl. Phys. 24, Supplement 24-2, pp. 284-286, 1985.
8. H. Adachi, T. Mitsuyu and K. Wasa, SAW properties of PLZT epitaxial thin films, Jap. J. Appl. Phys. 24, Supplement 24-1, pp. 121-123, 1984.
9. H. Adachi, T. Mitsuyu, O. Yamazaki and K. Wasa, Bragg A-O deflector using a piezoelectric PLZT thin film, Jap. J. Appl. Phys. 24, Supplement 24-2, pp. 287-289, 1985.
10. C. E. Land, Longitudinal electrooptic effects and photosensitivities of lead zirconate titanate thin films, J. Am. Ceram. Soc., (in press).
11. C. E. Land, Optical information storage in PLZT thin films, Proceedings of the Symposium on Thick and Thin Films, Am. Ceram. Soc., (in press).
12. S. J. Martin, M. A. Butler and C. E. Land, Ferroelectric optical image comparator using PLZT thin films, Electronics Letters 24(24), pp. 1486-1487, November 1988.
13. C. E. Land and P. S. Peercy, A review of the effects of ion implantation on the photoferroelectric properties of PLZT ceramics, Ferroelectrics 45, pp. 25-43, 1982.
14. R. P. Freese, Optical disks become erasable, IEEE Spectrum 25(2), pp. 41-45, 1988.
15. C. E. Land, Bistable optical information storage using antiferroelectric-phase lead lanthanum zirconate titanate ceramics, J. Am. Ceram. Soc. 71(11), pp. 905-908, 1988.